Orazio Descalzi
Marcel Clerc
Stefania Residori
Gaetano Assanto *Editors*

Localized States in Physics: Solitons and Patterns

Springer

Localized States in Physics: Solitons and Patterns

Orazio Descalzi • Marcel Clerc • Stefania Residori
Gaetano Assanto
Editors

Localized States in Physics: Solitons and Patterns

Springer

Editors
Orazio Descalzi
Universidad de los Andes
Facultad de Ingeniería y Cs. Aplicadas
Av. San Carlos de Apoquindo 2200
Las Condes
Santiago
Chile
odescalzi@miuandes.cl

Marcel Clerc
Universidad de Chile
Fac. de Cs. Físicas y Mat.
Depto. de Física
Casilla 487 - 3
Santiago
Chile
marcel@dfi.uchile.cl

Stefania Residori
Institut Non-linéaire de Nice
route de Lucioles 1361
06560 Valbonne
France
stefania.residori@inln.cnrs.fr

Gaetano Assanto
University Roma Tre
Nonlinear Optics and OptoElectronics Lab
Via della Vasca Navale 84
00146 Roma
Italy
assanto@uniroma3.it

ISBN 978-3-642-16548-1 e-ISBN 978-3-642-16549-8
DOI 10.1007/978-3-642-16549-8
Springer Heidelberg Dordrecht London New York

Cover design: eStudio Calamar S.L.

Printed on acid-free paper

Springer is part of Springer Science+Business Media (www.springer.com)

Preface

Physical systems driven far from thermodynamic equilibrium can give rise to a variety of dissipative spatial structures through spontaneous breaking of symmetries. A fascinating feature of these pattern-forming systems is their tendency to originate spatially confined states. Such localized states can exist as wave packets or propagating entities through space and/or time. Observed in many different branches of science, localized states appear to be ubiquitous in nature and characterized by common macroscopic properties, independently of the specific physical laws governing the underlying field and/or matter interactions. Even though Localized States in Physics can be found in such different domains as hydrodynamics, optics, granular matter, reaction-diffusion systems, neural networks, plasmas, Bose-Einstein condensates etc., books on the topic are still very rare and often devoted to a particular type. This Book is based on a series of lectures given at a workshop on the subject: it reflects the spirit and the breadth of the meeting, held in 2008 at the University of los Andes, Santiago, Chile. Its main motivations stem from the need to bring together - coolate and compare - various approaches to the description of localized states in physics, offering a comprehensive panorama of confined states, from localized patterns to solitons, convectons, oscillons, pulses, etc., aimed at establishing a common - or at least shared - comprehension of these physical states. In fluids, for instance, convecting regions can coexist stably with non-convecting regions in uniformly heated cells. Localized hexagonal patterns have also been observed in a parametrically excited layer of fluid. In chemical systems, autocatalytic reactions on metallic surfaces can lead to solitary waves with partial and full annihilation after collision of pulses traveling in opposite directions. In granular matter, vertically driven layers of particles (sand, rice, stones, metal balls, etc.) reveal that, for peak acceleration exceeding a critical value, standing wave patterns spontaneously form and oscillate at half the excitation frequency. Square, stripe, hexagonal and spiral patterns can emerge, depending on the oscillation frequency and amplitude of the forcing, including coherent states such as localized standing waves or oscillons. Localized states are also relevant in neural systems, where action potentials propagate along axons or networks of thalamic neurons exhibit activity waves, just to mention two examples. In optics, the interplay between dispersion/diffraction

and the medium nonlinearity leads to light propagation in space/time self-confined beams, the so-called optical solitons. In the presence of feedback, optical localized structures such as cavity solitons have been identified as transverse solutions encompassing bistability; they have been observed in several media and controlled by suitable addressing protocols. Finally, coherence and interference properties of atomic clouds of Bose-Einstein condensates, as well as localized structures in population models, have been investigated. The book covers quite a few of the most active and interesting contemporary aspects of Localized States in Physics, providing both review elements and current information on the latest research in the field. It consists of thirteen chapters discussing localized objects in optics, fluids and neural networks. The first four chapters are mostly dedicated to fundamental research in light localization. Reports on the state-of-the-art in optical spatial solitons, self-confined light and optical turbulence are presented with particular emphasis on experimental observations. The related theoretical work is treated in a general way and recent nonlinear optical experiments are reported to support the various predictions. The next three chapters deal with localized structures as localized solutions of pattern-forming systems. Analogies are drawn between fluids and optics, with a chapter dedicated to confined convective states in fluids and another one to optical transverse structures in liquid crystal light-valves. The recent theoretical developments in pattern localization are treated in a dedicated chapter, where crystal-like hexagonal structures are shown to localize according to the symmetry of the underlying grid. In the second part of the book special attention is paid to the potentials of localized states towards applications. Four chapters are devoted to optical systems and their use for controllable light pixels. Finally, excitability and localized states are treated in the last two chapters, where pulse localization is illustrated with examples in a nonlinear optical cavity and in neural networks. The Book as a whole is intended for an audience of senior and junior researchers and graduate students working in the field of pattern formation, instabilities and spatio-temporal dynamics of macroscopic systems far from equilibrium. It provides an overview of the state-of-the-art in localized states to a readership of physicists, mathematicians, electrical/electronic engineers. We trust that a number of scientists from neighbouring areas, such as e.g. biology, sociology, environment science and meteorology, will find its contents stimulating and informative.

Santiago de Chile,
August 2010

Orazio Descalzi
Marcel G. Clerc
Stefania Residori
Gaetano Assanto

Acknowledgements

We wish to thank the following national and international institutions for the their financial support, that made possible **Localized states in Physics: a focused workshop 2008**:

- Facultad de Ingeniería y Cs. Aplicadas, Universidad de los Andes, Chile.
- Fondo de Ayuda a la Investigación, Universidad de los Andes, Chile.
- Departamento de Física, Facultad de Cs. Físicas y Matemáticas, Universidad de Chile, Chile.
- Nonlinear Optics and OptoElectronics Lab, CNISM, University of Rome "Roma Tre", Italy.
- Institut Non Linéaire de Nice, France.
- The Center for Advanced Interdisciplinary Research in Materials – CIMAT (Chile).
- The Consortium of the Americas for Interdisciplinary Science, University of New Mexico (USA).
- Programa Bicentenario de Ciencia y Tecnología, Anillo ACT 15, "Dynamics, Singularities and Geometry of Matter out of Equilibrium".

Contents

Part II Localized structures in pattern forming systems

Part III Localized structures for optical applications

List of Contributors

Miroslaw A. Karpierz
Faculty of Physics, Warsaw University of Technology, Koszykowa 75, 00662 Warsaw-Poland, e-mail: karpierz@if.pw.edu.pl

Gaetano Assanto
NooEL, Nonlinear Optics and OptoElectronics Lab, CNISM, University of Rome "Roma Tre", Via della Vasca Navale 84, 00146 Rome - Italy, e-mail: assanto@uniroma3.it

Mousa Ayoub
Institut für Angewandte Physik and Center for Nonlinear Science, Westfälische Wilhelms-Universität Münster, Corrensstr. 2/4, 48149 Münster, Germany, e-mail: Ayoubm@uni-muenster.de

Björn Gütlich
Institut für Angewandte Physik and Center for Nonlinear Science, Westfälische Wilhelms-Universität Münster, Corrensstr. 2/4, 48149 Münster, Germany

Cornelia Denz
Institut für Angewandte Physik and Center for Nonlinear Science, Westfälische Wilhelms-Universität Münster, Corrensstr. 2/4, 48149 Münster, Germany, e-mail: denz@uni-muenster.de

Francesco Papoff
SUPA, Department of Physics, University of Strathclyde, 107 Rottenrow, Glasgow, G4 0NG, Scotland, U.K. e-mail: papoff@phys.strath.ac.uk

Gian-Luca Oppo
SUPA, Department of Physics, University of Strathclyde, 107 Rottenrow, Glasgow, G4 0NG, Scotland, U.K. e-mail: gianluca@phys.strath.ac.uk

William Firth
SUPA, Department of Physics, University of Strathclyde, 107 Rottenrow, Glasgow, G4 0NG, Scotland, U.K. e-mail: willie@phys.strath.ac.uk

Umberto Bortolozzo
INLN, Université de Nice Sophia-Antipolis, CNRS, 1361 route des Lucioles 06560 Valbonne, France e-mail: Umberto.Bortolozzo@inln.cnrs.fr

Marcel G. Clerc
Departamento de Física, Facultad de Ciencias Físicas y Matemáticas, Universidad de Chile, Casilla 487-3, Santiago, Chile, e-mail: marcel@galileo.dfi.uchile.cl

René G. Rojas
Instituto de Física, Pontificia Universidad Católica de Valparaíso, Casilla 4059, Valparaíso, Chile e-mail: rene.rojas@ucv.cl

Florence Haudin
INLN, Université de Nice Sophia-Antipolis, CNRS, 1361 route des Lucioles 06560 Valbonne, France e-mail: Florence.Haudin@inln.cnrs.fr

Stefania Residori
INLN, Université de Nice Sophia-Antipolis, CNRS, 1361 route des Lucioles 06560 Valbonne, France, e-mail: Stefania.Residori@inln.cnrs.fr

Daniel Escaff Dixon
Complex Systems Group, Facultad de Ingeniería y Cs. Aplicadas, Universidad de los Andes, Av. San Carlos de Apoquindo 2200, Santiago, Chile e-mail: descaff@uandes.cl

Giovanna Tissoni
CNISM and INFM–CNR, Dipartimento di Fisica e Matematica, Università dell'Insubria, Como, Italy e-mail: giovanna.tissoni@uninsubria.it

Franco Prati
CNISM and INFM–CNR, Dipartimento di Fisica e Matematica, Università dell'Insubria, Como, Italy e-mail: franco.prati@uninsubria.it

Luigi A. Lugiato
CNISM and INFM–CNR, Dipartimento di Fisica e Matematica, Università dell'Insubria, Como, Italy e-mail: luigi.lugiato@uninsubria.it

Keivan M. Aghdami
Physics Department, Payame Noor University, Mini City, 19569 Tehran, Iran

Massino Brambilla
INFM–CNR, Dipartimento di Fisica Interateneo, Politecnico di Bari, Italy e-mail: m.brambilla@poliba.it

Arantxa Alonso
Departament de Física Aplicada, Universitat Politècnica de Catalunya, Barcelona, Spain e-mail: arantxa@fa.upc.edu

Oriol Batiste
Departament de Física Aplicada, Universitat Politècnica de Catalunya, Barcelona, Spain e-mail: oriol@fa.upc.edu

Isabel Mercader
Departament de Física Aplicada, Universitat Politècnica de Catalunya, Barcelona, Spain e-mail: isabel@fa.upc.edu

Edgar Knobloch
Department of Physics, University of California, Berkeley CA 94720, USA e-mail: knobloch@berkeley.edu

Damià Gomila
IFISC, Instituto de Física Interdisciplinar y Sistemas Complejos (CSIC-UIB), Campus Universitat Illes Balears, 07122 Palma de Mallorca, Spain, e-mail: damia@ifisc.uib-csic.es

Adrián Jacobo
IFISC, Instituto de Física Interdisciplinar y Sistemas Complejos (CSIC-UIB), Campus Universitat Illes Balears, 07122 Palma de Mallorca, Spain, e-mail: jacobo@ifisc.uib-csic.es

Manuel A. Matías
IFISC, Instituto de Física Interdisciplinar y Sistemas Complejos (CSIC-UIB), Campus Universitat Illes Balears, 07122 Palma de Mallorca, Spain, e-mail: manuel.matias@ifisc.uib-csic.es

Pere Colet
IFISC, Instituto de Física Interdisciplinar y Sistemas Complejos (CSIC-UIB), Campus Universitat Illes Balears, 07122 Palma de Mallorca, Spain, e-mail: pere@ifisc.uib-csic.es

Dmitry V. Dylov
Department of Electrical Engineering, Princeton University, Olden Street, Princeton, New Jersey 08544, USA e-mail: dvd@princeton.edu

Jason W. Fleischer
Department of Electrical Engineering, Princeton University, Olden Street, Princeton, New Jersey 08544, USA e-mail: jasonf@princeton.edu

Richard S. Tasgal
Departments of Chemistry and Electro-Optics, and the Ilse Katz Center for Nano-Science, Ben-Gurion University of the Negev, Beer-Sheva 84105, Israel e-mail: tasgal@gmail.com

Roman Shnaiderman
Departments of Chemistry and Electro-Optics, and the Ilse Katz Center for Nano-Science, Ben-Gurion University of the Negev, Beer-Sheva 84105, Israel e-mail: rshnaider@gmail.com

Yehuda B. Band
Departments of Chemistry and Electro-Optics, and the Ilse Katz Center for Nano-Science, Ben-Gurion University of the Negev, Beer-Sheva 84105, Israel e-mail: band@bgu.ac.il

Jason Laurie
Mathematics Institute, University of Warwick, Coventry CV4 7AL, United Kingdom e-mail: J.P.Laurie@warwick.ac.uk

Sergey Nazarenko
Mathematics Institute, University of Warwick, Coventry CV4 7AL, United Kingdom e-mail: S.V.Nazarenko@warwick.ac.uk

Massimo Giudici
Université de Nice Sophia Antipolis, Centre National de la Recherche Scientifique, Institut Non Linéaire de Nice, 1361 route des lucioles, Valbonne, France e-mail: Massimo.Giudici@inln.cnrs.fr

Francesco Pedaci
Université de Nice Sophia Antipolis, Centre National de la Recherche Scientifique, Institut Non Linéaire de Nice, 1361 route des lucioles, Valbonne, France

Emilie Caboche
Université de Nice Sophia Antipolis, Centre National de la Recherche Scientifique, Institut Non Linéaire de Nice, 1361 route des lucioles, Valbonne, France

Patrice Genevet
Université de Nice Sophia Antipolis, Centre National de la Recherche Scientifique, Institut Non Linéaire de Nice, 1361 route des lucioles, Valbonne, France e-mail: patrice.genevet@inln.cnrs.fr

Stephane Barland
Université de Nice Sophia Antipolis, Centre National de la Recherche Scientifique, Institut Non Linéaire de Nice, 1361 route des lucioles, Valbonne, France

Jorge Tredicce
Université de Nice Sophia Antipolis, Centre National de la Recherche Scientifique, Institut Non Linéaire de Nice, 1361 route des lucioles, Valbonne, France e-mail: Jorge.Tredicce@inln.cnrs.fr

Jaime E. Cisternas
Complex Systems Group, Facultad de Ingeniería y Ciencias Aplicadas, Universidad de los Andes, Santiago, Chile e-mail: jecisternas@miuandes.cl

Thomas M. Wasylenko
Department of Chemical Engineering, Princeton University, Princeton, U.S.A. Current address: Department of Chemical Engineering, Massachusetts Institute of Technology, Cambridge, U.S.A. e-mail: twasylen@mit.edu

Ioannis G. Kevrekidis
Department of Chemical Engineering and Program of Applied and Computational Mathematics, Princeton University, Princeton, U.S.A. e-mail: yannis@princeton.edu

Part I
Solitons, self-confined light and optical turbulence

Chapter 1
Light Self-trapping in Nematic Liquid Crystals

Miroslaw A. Karpierz and Gaetano Assanto

Abstract We review the most important achievements and recent progress in the area of light-beam self-localization into optical spatial solitons in reorientational molecular media, with specific focus on nematic liquid crystals in planarly aligned, twisted and chiral arrangements.

1.1 Introduction

Liquid crystals are widely used in displays for a large and ever growing number of applications, including high resolution television sets. It is less known to the general public that these molecular materials are employed and studied with a much larger set of scientific objectives, including electro-optic modulators and nonlinear photonics, particularly in devices for light switching and all-optical circuits towards novel generations of optical telecom systems. These molecular dielectrics are fluid, transparent, damage resistant, temperature and voltage tunable, etc. [1, 2, 3]. When the organic molecules, typically large and rod-shaped, are ordered in the so-called nematic phase, liquid crystals tend to exhibit a large (optical and radio-frequency) birefringence and their optical properties can also be modified by light through a nonlinear reorientational response, i.e. their constituent organic molecules can rotate and reorientate in space based on the optical excitation [1, 2, 3]. The latter nonlinear response is known as optical reorientation and has been exploited to investigate light-beam self-localization in non-diffracting filaments or spatial solitons, i.e. beams which do not spread upon propagation, maintain an invariant transverse

Miroslaw A. Karpierz
Faculty of Physics, Warsaw University of Technology, Koszykowa 75, 00662 Warsaw-Poland
e-mail: karpierz@if.pw.edu.pl

Gaetano Assanto
NooEL, Nonlinear Optics and OptoElectronics Lab, CNISM, University of Rome "Roma Tre"
Via della Vasca Navale 84, 00146 Rome - Italy, e-mail: assanto@uniroma3.it

O. Descalzi et al. (eds.), *Localized States in Physics: Solitons and Patterns*,
DOI 10.1007/978-3-642-16549-8_1, © Springer-Verlag Berlin Heidelberg 2011

profile via a power-driven increase in refractive index and are able to guide weaker signals [4, 5, 6, 7]. The molecular nonlinearity of nematic liquid crystals (NLC) is large (i.e. it requires low powers), depends on field polarization but is substantially independent on wavelength in the whole transparency range, typically from visible to mid-infrared; being associated to molecular motion in a fluid, it is rather slow in time, this latter drawback requiring a careful choice/selection of potential applications in reconfigurable circuits. The light-driven NLC reorientational response supports various phenomena [2, 3] and, as anticipated, the generation and propagation of stable and robust self-trapped spatial solitary waves, also named Nematicons [4]. The first solitons in NLC were observed in hollow capillaries filled with dye-doped materials [8, 9, 10]; they exploited the thermal response through absorption and, in some cases, a phase transition from nematic to isotropic states. Recently, the most studied geometries for optical solitons have been planar cells with non-absorbing NLC, various boundary conditions and applied voltage biases. In the next section we give a brief account of the basics of the reorientation response and the excitation of nematicons. In Section 11.3 we overview the main recent results on nematicons in undoped nematic liquid crystals in planar geometries. In Section 7.4 we discuss spatial optical solitons in twisted and chiral NLC.

1.2 Reorientational Self-focusing in Nematic Liquid Crystals

Optical reorientation in nematic liquid crystals relies on the structure of the medium, which consist of anisotropic elongated non-polar molecules in a fluid state [1]. In the isotropic phase these molecules are disordered in position and orientation, the latter usually defined by the angle of their major axis or director **n**, a unity vector corresponding to the optic axis. In the nematic phase, the NLC director exhibits an average angular orientation, typically mediated by molecular anchoring at the boundaries of a cell. The director distribution in an NLC cell can be modified by anchoring at the surfaces, applied electromagnetic fields, medium temperature, light beams. NLC, in fact, maintain their fluid state despite the anchoring, with changes in director orientation related to the free energy of density:

$$f_{\mathrm{F}} = \frac{1}{2}K_{11}\left(\nabla\cdot\mathbf{n}\right)^2 + \frac{1}{2}K_{22}\left(\mathbf{n}\cdot\nabla\times\mathbf{n}+G\right)^2 + \frac{1}{2}K_{33}\left(\mathbf{n}\times\nabla\times\mathbf{n}\right)^2, \qquad (1.1)$$

with K_{ii} the elastic (Frank) constants for the three basic spatial distortions of the molecules: splay (K_{11}), twist (K_{22}) and bend (K_{33}). In most common NLC $K_{33} > K_{11} > K_{22}$ and are of the order of a few pN units [1, 2, 3]. Expression (1) is often simplified by taking $K_{11} = K_{22} = K_{33} = K$. The parameter G in the second term on the RHS of (1) describes chirality with pitch p: $G = 0$ for standard NLC and $G = 2\pi/p$ for chiral nematic liquid crystals (ChNLC). Owing to the elongated shape of molecules in NLC, valence electrons have a larger mobility along the major axis; hence, the dielectric permittivity is higher for field vectors parallel to **n**. In the nematic phase, therefore, typical NLC are birefringent dielectrics with uni-

axial properties, i. e. $\Delta\varepsilon = \varepsilon_{\parallel} - \varepsilon_{\perp}$, $\varepsilon_{\parallel}$ and $\varepsilon_{\perp}$ being the components of the electric permittivity (at low and/or optical frequencies) for extraordinary and ordinary polarizations, respectively. An electric field $\mathbf{E}$, either externally applied (e.g. a voltage) or associated to a propagating light beam, can rotate the main molecular axis by a Coulombian torque, the latter trying to align $\mathbf{n}$ along the field vector despite anchoring at the boundaries and the free energy (1). This latter interaction energy has density

$$f_{\mathrm{el}} = -\frac{\varepsilon_0 \Delta\varepsilon}{2} \left\langle (\mathbf{n}\cdot\mathbf{E})^2 \right\rangle \tag{1.2}$$

Since energy (2) is minimized when $\mathbf{n}$ is parallel to the $\mathbf{E}$ field vector, the reorientational response is a saturable one: the maximum nonlinearity corresponds to a change from $\varepsilon_{\perp}$ to $\varepsilon_{\parallel}$ or from ordinary index $n_{\perp}$ to extraordinary index $n_{\parallel}$. An intense enough extraordinarily polarized beam, such that $\mathbf{E}$, propagation wavevector $\mathbf{k}$ and NLC optic axis $\mathbf{n}$ are coplanar, can alter the molecular orientation, increase the electric permittivity and the extraordinary index of refraction, give rise to self-focusing. Such effect can be modeled by deriving the Euler-Lagrange-Rayleigh equations from the minimization of the total free energy, which includes the deformation energy, the interaction energy with external fields, the interaction energy with the boundaries and the dissipation energy [7]. The latter has density f_{R}

$$f_{\mathrm{R}} = \frac{1}{2}\gamma \left(\frac{\partial \mathbf{n}}{\partial t} \right)^2 \tag{1.3}$$

with γ the orientational viscosity. The density f_{R} is required in time-dependent analyses.

When the director at the boundaries and the electric field $\mathbf{E}$ lie in the same plane, the angle θ defining the orientation of the director $\mathbf{n}$ with respect to the propagation coordinate z can describe the reorientation in two-dimensional problems, as sketched in Fig. 1.1. The refractive index for an extraordinarily polarized field varies with θ according to the usual

$$n_{\mathrm{e}}(\theta) = \frac{n_{\perp} n_{\parallel}}{\sqrt{n_{\perp}^2 \cos^2\theta + n_{\parallel}^2 \sin^2\theta}} \tag{1.4}$$

For the geometry sketched in Fig. 1.1 the director $\mathbf{n} = (\sin\theta, 0, \cos\theta)$. Assuming an initial orientation $\theta = \theta_0$, nonlinear beam propagation at wavelength λ (frequency ω) is ruled by the coupled system

$$4K\nabla_{\perp}^2\theta + \varepsilon_0 \Delta\varepsilon \sin(2\theta)|A|^2 = 0 \tag{1.5}$$

$$2ik\frac{\partial}{\partial z}A + \nabla_{\perp}^2 A + \frac{\omega^2}{c^2} n_{\mathrm{e}}^2(\theta) A - k^2 A = 0 \tag{1.6}$$

with A the slowly-varying beam envelope, $\nabla_{\perp}^2 = \partial^2/\partial x^2 + \partial^2/\partial y^2$ the Laplacian in the transverse plane, $k \approx (\omega/c)\sqrt{n_{\perp}^2 + \Delta\varepsilon \sin^2\theta_0}$, c the light speed in vacuum [11].

Eq. (6) is a saturable (θ cannot exceed $\pi/2$) nonlinear Schrödinger-like equation with an index increase limited by $\Delta n = n_{\parallel} - n_{\perp}$. In Eq. (5) and Eq. (6), the initial value θ_0 can represent the effect of a fixed pre-tilt or a tilt induced by a voltage V applied to the NLC thickness across x. A small initial tilt, such that **n** and **E** are not perpendicular to one another, prevents the threshold effect known as Fréedericksz transition. Eq. (6) holds valid with $\theta_0 = constant$ for narrow beams in thick cells, i. e., in NLC regions far from the anchoring boundaries. System (5)-(6) models a nonlocal nonlinear response, whereby the reorientational index change extends beyond the transverse size of the beam field envelope [12]. Nonlocality, as well as saturation, allow nematicons to be stable and robust in 2+1 dimensions [13, 14]. Fig. 1.1(b) displays the calculated distribution of $\theta(x)$ as compared to a bell-shaped electric field excitation for various intensities I_0. It is apparent that the boundary conditions affect the nonlocal response and its strength depending on the waist of the beam [5, 15, 16].

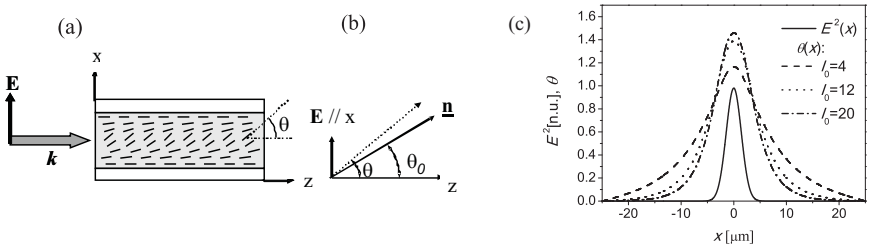

Fig. 1.1 (a) Geometry of a bounded NLC layer in a planar cell with voltage bias across the thickness. (b) The input **E** field belongs to the principal plane xz and is coplanar with **n** and $\mathbf{k} \parallel \mathbf{z}$. (c) Distribution of $\theta(x)$ for various electric field excitations. The field profile is the solid curve. In this 1D calculations we used an NLC layer thickness of 50 μm and boundary conditions $\theta(-d/2) = \theta(d/2) = 0.01$

The reorientational response of NLC, stemming from the shape of the constituent non polar molecules determines the properties of spatial optical solitons. The nonlinearity is polarization sensitive, self-focusing, saturable, non instantaneous and nonlocal; hence, it supports stable two-dimensional propagating solitons. Moreover, owing to the refractive index increase counterbalancing diffraction, co-polarized signals of different wavelengths can be guided within the soliton channels [11, 17]. By using the correct input beam polarization, applying suitable boundary conditions at the interfaces containing the layer of NLC, e.g. by mechanical rubbing, appropriate pre-tilt θ_0 can maximize the nonlinear response and allow mW power excitations to generate nematicons with propagation over several Rayleigh distances, i. e. to define reconfigurable signal interconnects. In the remaining of this chapter we will illustrate the main properties of low-power reorientational nematicons in threshold-less configurations.

Nematicons have been investigated in various cell geometries, from hollow capillaries to thick cells with fiber in/out connections, to thin planar waveguides. The main planar cells for 2D nematicons are sketched in Fig. 1.2 and consist of glass

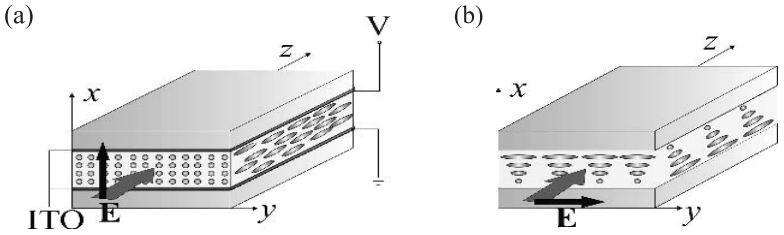

Fig. 1.2 Most common NLC planar cells for the study of optical spatial solitons: (a) planar anchoring with external voltage bias V applied by means of Indium Tin Oxide (ITO) thin film electrodes, (b) twisted or chiral NLC arrangement. The wide arrows along z indicate the excitation field wavevector of amplitude **E**, the thinner arrows refer to the input linear polarization

plates with proper rubbing at the internal interfaces [11]. The plates are held parallel and separated by spacers. Thin film transparent electrodes (e.g. Indium Tin Oxide) can be used to apply the desired low-frequency bias and tune the initial orientation θ_0. Input and output glass slabs can also be used to seal the cells and avoid meniscus formation and beam depolarization. When the NLC thickness is much larger than the waist of the input beam, the NLC layer can be treated as a bulk and the observation of (2+1) dimensional spatial solitons is possible [4, 7, 11, 13]. Conversely, if the thickness is comparable with the beam waist, then the structure is better modelled as a planar waveguide and can support (1+1) dimensional nematicons [5, 6].

1.3 Spatial Optical Solitons in Purely Nematic Liquid Crystals

The basic geometry adopted for demonstrating Nematicons in a planar glass cell containing undoped NLC (specifically, the Merck mixture known as E7) is sketched in Fig. 1.1(a) and Fig. 1.2(a) [7, 11]. The excitation was a linearly polarized Gaussian beam with the electric field parallel to x, i.e. extraordinarily-polarized. Surface anchoring and applied voltage across the $d = 75$ μm thickness guaranteed a threshold-less all-optical response in the uniaxial dielectric, as described by Eq. (4) and Eq. (5). In the presence of the external bias $V = dE_{\rm rf}$, neglecting walk-off in the plane xz and non-paraxial effects, the evolution of the slowly-varying beam amplitude A propagating along z in the mid-plane of the cell is modelled by [7, 11]:

$$2ik\frac{\partial}{\partial z}A + \nabla_\perp^2 A + \frac{\omega^2}{c^2}\left(n_\parallel^2 - n_\perp^2\right)\left(\sin^2\theta - \sin^2\theta_0\right)A = 0 \quad (1.7)$$

$$K\frac{\partial^2\theta}{\partial z^2} + K\nabla_\perp^2\theta + \frac{1}{2}\Delta\varepsilon_{\rm RF}E_{\rm rf}^2\sin(2\theta) + \frac{1}{4}\varepsilon_0\left(n_\parallel^2 - n_\perp^2\right)|A|^2\sin(2\theta) = 0 \quad (1.8)$$

with θ_0 the pre-tilt and θ the director orientation due to both light and voltage, $\Delta\varepsilon_{\rm RF}$ the dielectric anisotropy in the low frequency region.

System (7), for narrow nematicons with respect to the cell and small waist compared to the extent of the nonlocal response, reduces to a saturable nonlinear Schrödinger equation with nonlocal and stable 2D+1 self-localized solutions [12]. In this limit, nematicons exhibit the features attributed to "accessible" solitons by Snyder and Mitchell [14], with a breathing character resulting in the (quasi) periodic oscillation of their waist and peak intensity [12, 13, 14]. This breathing is excitation-dependent and can be reduced by exciting the solitons with power and waist close to their existence curve. In several experimental scenarios, nematicons often appear as transversely invariant beams with a slowly decaying intensity due to Rayleigh scattering in the medium. Self-localized solutions in the "local" regime can also be found for beams of waist comparable to the nonlocal range [18, 19]. Fig. 1.3(a) displays actual (colour-coded) images of individual 2mW Gaussian green (514.5nm) beams in the ordinary (top panel) and extraordinary (bottom) polarizations, resulting in linear (diffraction) and nonlinear (self-localized) propagation, respectively, as observed by collecting the out-of-plane scattered photons with a camera. The linear behaviour in the ordinary polarization corresponds to an **E**-field orthogonal to **n**; hence, to lack of reorientation below the Freedericks threshold. The nematicon (Fig. 1.3(a, lower panel) remains invariant over distances exceeding 20 diffraction lengths. Fig. 1.3(c) shows the corresponding evolution of a red (632.8 nm) probe (signal) co-polarized and co-launched with the pump: as a nematicon is generated, the weak signal is confined in the soliton waveguide despite its longer wavelength: another demonstration of the nonlocal nature of nematicons, inasmuch as the numerical aperture of the solitary channel exceeds that associated to the spatial extent of the self-localized solution.

Another effect of nonlocality is low-pass filtering. In the case of spatial incoherent excitations, e.g. a speckled beam produced by a diffuser, nonlocality can eliminate the high frequency wave-vector components and allow a spatial soliton to be formed, even if at the price of a larger power [20, 21, 23]. Fig. 1.3(b) and Fig. 1.3(d) display diffraction and self-localization of pump (Fig. 1.3(b)) and probe (Fig. 1.3(d)) in ordinary (top panels) and extraordinary (bottom) polarizations, respectively. It is apparent that an excitation of 2.7 mW (versus 2.0 mW in the coherent case) suffices to compensate the larger diffraction associated to the speckled input.

The incoherent character of nonlocal solitons also allows the formation of vector nematicons with two (or more) co-polarized wavelength components [24, 25], as well as the mutual attraction between nematicons, propagating either in plane [26, 27, 28] or out of plane [29, 30, 31, 32]. Fig. 1.4 illustrates a couple of simple in plane interactions between two solitons excited by equi-power beams propagating at a small angle. Since the initial separation does not exceed the nonlocal range, the nematicons tend to attract as the refractive perturbation links the two self-induced waveguides, until the in initially diverging beams become parallel (Fig. 1.4(b)). At higher input powers (Fig. 1.4(c)) the mutual attraction becomes strong enough to make the two solitons cross and interleave, exchanging their position along y. This power-dependent interaction can be exploited for all-optical switching and logic gates.

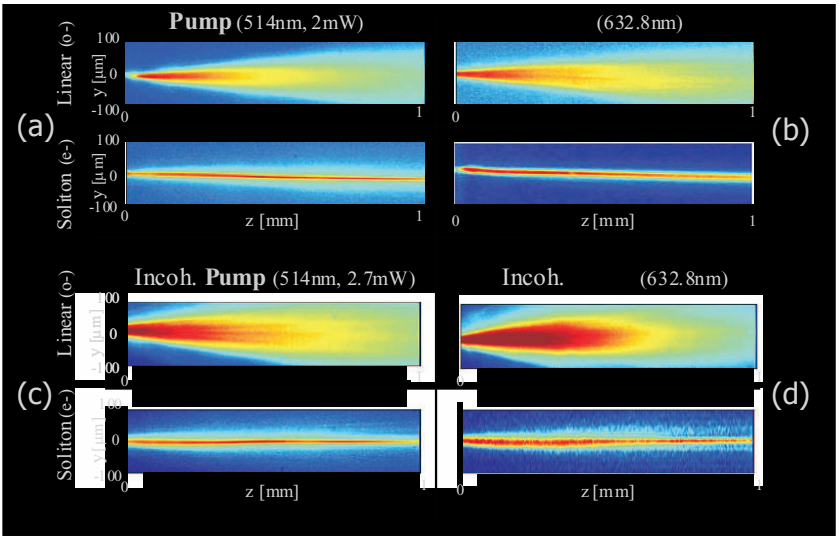

Fig. 1.3 Colour coded images of beam propagation from an Ar^+ laser (left) and a collinear co-polarized He-Ne laser (right) in a planar NLC cell with E7. (a) Top row: linear diffraction when injecting an ordinary polarization. Bottom: soliton propagation in the extraordinary polarization ($\| \mathbf{x}$); (b) corresponding linear (top) and nonlinear (bottom) evolution of the probe (100 μW). (c-d) Spatially incoherent beam propagation as in (a) and (b), respectively, but for a (c) 2.7 mW pump and (d) an equally incoherent probe

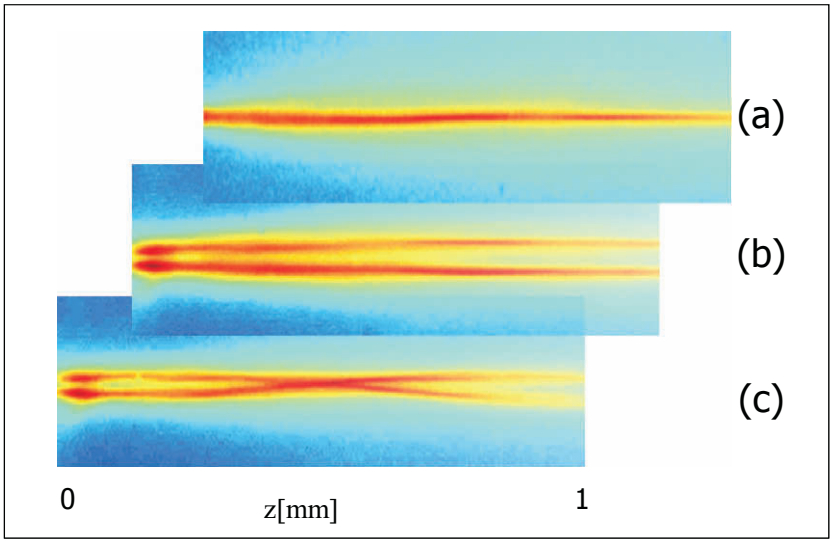

Fig. 1.4 Color coded images of (a) a single nematicon in a planar cell; (b) two identical nematicons launched by ≈2 mW beams forming a mutual angle of 1.7^o; (c) same as in (b) but with launch powers ≈4 mW

Figure 1.5 summarizes a few other cases of interactions between nematicons. If the initial separation and/or angle are large enough, the two spatial solitons cross each other (Fig. 1.5(a)) while maintaining straight trajectories, as for one-dimensional Kerr solitons [21]. Fig. 1.5(b) illustrates the formation of a few nematicons using a wide beam focused well inside the cell [33]: transverse modulational instability mediates the formation of a number of solitons depending on the size and power of the optical excitation [22, 34, 35]. Several nematicons can also be the by-product of a dispersive shock wave or undular bore [36]. Fig. 1.5(c) illustrates the interaction of two equi-power solitons lauched skew in the cell: mutual attraction gives rise to a cluster of nematicons with spiralling trajectories and angular momentum. Since the latter is proportional to the photon content of each soliton, as the excitation increases the cluster rotates faster, as displayed in Fig. 1.5(d) showing the output images of the two light spots versus input power [30, 31]. A similar behaviour has been also predicted with clusters of nematicons of different wavelengths and with more than two components.

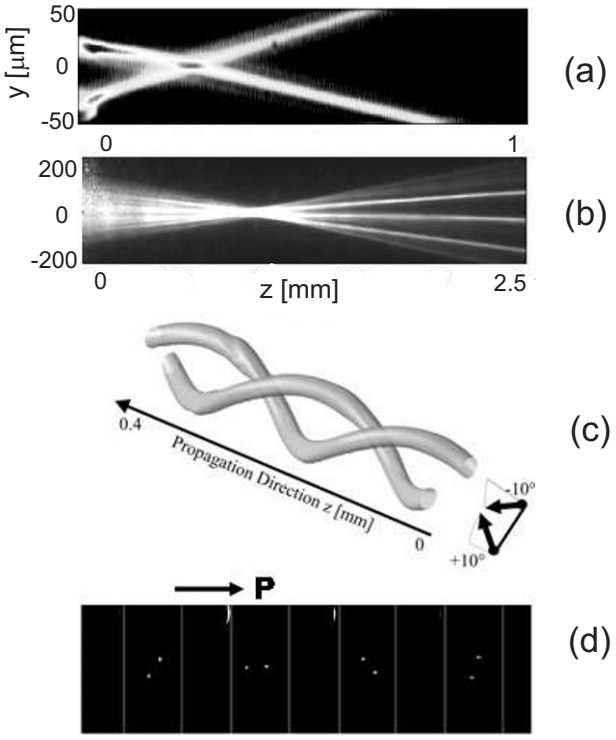

Fig. 1.5 (a) In plane crossing of two identical nematicons. (b) Multiple soliton generation by a focused light beam. (c) Out-of-plane attraction between two skew nematicons. (d) The photographs taken at the output of the cell show that, as the excitation increases, the cluster rotates faster in propagation, with a power-dependent angular change (π , in this set)

Nematicons are extraordinarily polarized wave-packets in uniaxials; hence, they undergo walk-off, i. e. their photon flux forms an angle

$$\delta(\theta) = \tan^{-1}\left(\frac{\left(n_{\parallel}^2 - n_{\perp}^2\right)\sin(2\theta)}{n_{\parallel}^2 + n_{\perp}^2 + \left(n_{\parallel}^2 - n_{\perp}^2\right)\cos(2\theta)}\right) \tag{1.9}$$

with the wave-vector. Such angle can be as large as $7-9^{o}$ in typical NLC, and suitable launch conditions need be adopted to prevent or reduce it not to make the soliton hit the cell boundaries [37]. Boundaries contribute to define the potential landscape for soliton propagation and can play an important role in the actual nematicon path within finite cells [38, 39, 40]. Since walk-off depends on the angle θ which, in turn, can be controlled by the external bias, the applied voltage can also be used to change nematicon trajectory by varying δ , either in the whole cell or in specific regions of it [41, 42, 43, 44]. In the latter case, graded interfaces can be formed and support soliton refraction or total internal reflection [43, 44]. Examples of refraction and total internal reflection in a cell with two electrodes defining regions of higher and lower optical densities are shown in Fig. 1.6 (a-b). Analogous effects can be obtained by illuminating NLC regions and inducing reorientation along the path of the nematicon. This has been demonstrated with lens-like perturbations in undoped NLC and Azo-NLC [45, 46], through dye-mediated absorption and surface anchoring [47], in liquid crystal light valves by means of a photoconductive layer altering the voltage drop across the NLC [48]. Finally, owing to the large walk-off, double refraction in uniaxial NLC can originate negative refraction at the input glass-NLC interface, with the soliton propagating in the same half-plane of the incident wave vector, as visible in Fig. 1.6(c) comparing ordinary and extraordinary (self-confined) beam propagation [49].

1.4 Spatial Optical Solitons in Chiral Nematic Liquid Crystals

In twisted and chiral nematic cells the molecular director is parallel to the glass plates (interfaces) and twisted within the film thickness (Fig. 1.2(b)) [50, 51]. Such an orientation is typically induced by the boundary conditions (in twisted nematics, TNLC) and by the chiral properties (in cholesteric liquid crystals, ChNLC). For light polarized along y the refractive index varies across the sample thickness from the ordinary value $n_{\perp}$ in planes where $\theta = 0$ to the extraordinary $n_{\parallel}$ in planes where $\theta = \pi/2$. A self-trapped light beam propagates in the thin layer where the refractive index is the largest (close to $n_{\parallel}$). In ChNLC several such layers occur throughout the liquid crystal and their number depends on the chirality pitch and the thickness of the film.

In the configurations investigated a light beam propagates in the z-direction parallel to the glass plates and is initially linearly polarized with the electric field vector $\mathbf{E} = \mathbf{y}E_{\mathrm{y}}$ also parallel to the interfaces. Because the birefringence axis rotates across

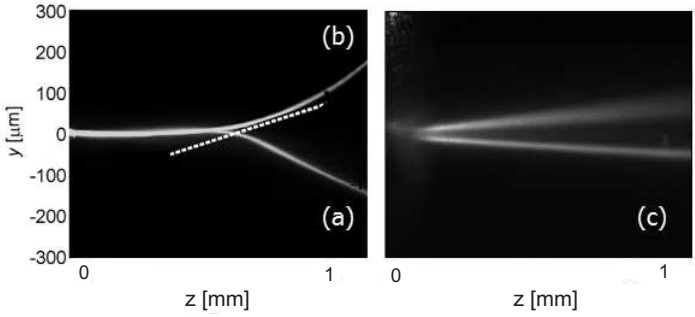

Fig. 1.6 (a-b) A planar cell with suitable director orientation in the plane yz and two sets of electrodes can be used to define two dielectric regions separated by a graded interface (dashed line). If the nematicon, injected from the left, reaches the interface from an optically rarer region, it can undergo refraction as in (a). If the input region is denser, the soliton can undergo total internal reflection, as in (b). The overall change in angle from refraction to reflection in this experiment is $18+22=40^{\circ}$. (c) Double refraction in NLC: the ordinary beam component (upper) undergoes positive refraction while diffracting; the extraordinary beam nematicon propagates with negative refraction (towards $y<0$) at the walk-off angle with respect to **k** (along the ordinary beam)

the layer, during propagation all components of electric and magnetic fields appear. However, only E_{y} and E_{z} are important for reorientation. Using the Euler-Lagrange equation for energy minimization, the following partial differential equation can be obtained:

$$K\frac{\partial^2\theta}{\partial x^2}+\frac{1}{4}\varepsilon_0\Delta\varepsilon\left[\left(|E_{\mathrm{z}}|^2-\left|E_{\mathrm{y}}\right|^2\right)\sin(2\theta)+\left(E_{\mathrm{y}}^*E_{\mathrm{z}}+E_{\mathrm{z}}^*E_{\mathrm{y}}\right)\cos(2\theta)\right]=0 \quad (1.10)$$

where $\theta(x)=\theta_0+2\pi x/p$ is the initial orientation (without electric field) and p is the chirality pitch. The description of light propagation in a twisted or a chiral NLC layer can be simplified by assuming that the beam profile along x is roughly constant, a hypothesis which is correct at some distance from the input, where the self-guided mode is formed. In this limit, taking $E_{\mathrm{z}}<<E_{\mathrm{y}}$, the slowly varying amplitude A is ruled by [50, 51]:

$$2\mathrm{i}\beta\frac{\partial}{\partial z}A-\frac{\partial^2}{\partial y^2}\gamma_1 A+2\mathrm{i}\beta\frac{\partial}{\partial y}\gamma_2 A-\beta^2\left(\gamma_1-\gamma_1^{(0)}\right)=0 \quad (1.11)$$

where β is the propagation constant of the planar waveguide mode and the coefficients γ_1 and γ_2 depend on the orientation angle ($\gamma_1^{(0)}$ is the value of γ_1 for the initial orientation). These coefficients have a saturable form and can be calculated for any specific liquid crystal layer. γ_2 is connected with the walk-off of the light beam when the latter is asymmetrically launched into the film. γ_1 relates to nonlinearity and is responsible for self-focusing and the creation of spatial solitons. The